GLORIA M. MONSALVE-BRAVO*, H. MARCELA MOSCOSO-VASQUEZ, HERNAN ALVAREZ
*Corresponding Author
Universidad Nacional de Colombia, Facultad de Minas, Departamento de Procesos y Energía, Medellín,
Carrera 80 # 65-223 - Núcleo Robledo, Colombia.


Gloria M. Monsalve-Bravo

Scale-up of continuous reactors
using phenomenological-based models

KEYWORDS: Hankel matrix, phenomenological-based model, operating point, scale-up methodology, dynamics hierarchy.

Abstract A methodology for scaling up continuous reactors using a Phenomenological-Based Semiphysical Model (PBSM) of the process is presented. First, a review of the most popular scale-up methods is made, finding that these methods do not guarantee an adequate commercial unit design and that a PBSM is a fundamental tool when scaling up chemical reactors. Taking into account these facts, a novel methodology is presented in which a process PBSM and its Hankel matrix are used for analysing the process dynamic behaviour and scaling it up, including the effect of the design variables over each state variable. Finally, the proposed methodology is applied to a polymerization reactor, comparing the scaled unit design when using this approximation and a traditional method, finding the scale factors for keeping the same polymer molecular weight at the new scale and, demonstrating that traditional scale-up methods do not always lead into the best commercial unit design.

INTRODUCTION

Although the scale-up activity is one of the major tasks for chemical engineers and represents a fundamental step in the design and optimization of industrial plants (1), since the 1960s there has not been significant progress in the methods for scaling up chemical reactors (use of rules of thumb, similarity criteria and dimensional analysis) (2-7). Industrial scale-up is dominated by empirical criteria that require geometrical similarity fulfilment, leading to drawbacks from keeping a single parameter constant (8, 9) and originating changes in other important variables. This fact results in an erroneous commercial unit design that demands additional costs and time to be corrected (10-12).

Considering the importance of processes scale-up in all industrial activities (1, 3, 4, 9), this work presents a novel methodology for scaling up continuous reactors using i) a Phenomenological-Based Semiphysical Model (PBSM) for representing the process, and ii) its Hankel matrix as a tool for establishing the process dynamics hierarchy and real scale factors, by means of the State Impactability Index (SII). The latter tool has been widely used in model reduction (13), systems identification, digital filter design (14), and controllers design when determining input-output pairings (15).

The paper is organized as follows. First, a brief review of the scale-up methods analysing their limitations is made. Then, the methodology for scaling up continuous processes is presented using both a process PBSM and Hankel matrix. Finally, the proposed methodology is applied to a methyl methacrylate (MMA) polymerization reactor, establishing the scaled unit design with the same Operating Point (OP) of the current scale and the dynamics hierarchy at both scales.

TRADITIONAL SCALE-UP METHODS AND SCALE-UP PROPOSED PROCEDURE

It is possible to distinguish three basic approaches in the scale-up procedure (5, 16). The first one is known as physical approach. This approach uses dimensionless numbers, variables and relations to relate the same process at different scales. Two different methods can be followed in the context of the physical approach (9, 17): i) similarity criteria which includes: a) geometrical, b) mechanical (static, kinematic and dynamic), c) thermal and d) chemical similarities (4, 18, 19), and ii) dimensional analysis which includes (6): a) Buckingham π-theorem based method and b) inspectional analysis that involves the dimensionless layout of the process governing equations (20).

The second one is the experimental approach, also called empirical approach. In this approach, the designer knowledge of a particular process is used for carrying out its scale-up (3, 8). Two different methods can be followed in the context of the experimental approach: i) trial and error, in which experimental process data are used for the construction of empirical relations (3, 21, 22) and ii) the use of rules of thumb that usually consider a constant value of a particular operating parameter as a general rule during the scale-up (8, 11, 23).

The third one is known as fundamental approach. This approach involves proper modelling of the process under consideration (11, 24). It is based in the development of a phenomenological-based model for the description of the process behaviour (5), generating an excellent process understanding and allowing for a process to be scaled-up more than a 1000 times, quickly and reliably (3, 21). Two different methods can be followed in the context of the fundamental approach: i) simulations with variation of parameters

(2, 11, 23) and ii) the use of the dynamics hierarchy (Hankel matrix). The latter is proposed in this work based on a previous methodology developed by Ruiz and Alvarez (3), but overcoming its limitations.
In practice, the previously described methods are indiscriminately combined when scaling up chemical processes, especially because geometrical similarly is usually taken as a primary criterion when designing a new operating unit (3, 5, 6, 21). Within the drawbacks of these scale-up methods, the main problem is to make a complete list of the relevant independent variables (7). Here science meets art: the choice of these variables is highly subjective, disregarding any rigor (6, 20). As mentioned in the physical approach, four similarity criteria must be considered in chemical engineering (geometrical, mechanical, thermal and chemical); each criterion requiring the fulfilment of the other ones. However, in real engineering problems it is impossible to satisfy the similarity criteria (as a whole), resulting in the fact that not all the characteristic parameters and not all the dimensionless numbers can be kept constant when scaling up a process. So, given that some parameters cannot be fixed, they may change substantially in unforeseen ways, altering process behaviour (10, 11).
On the other hand, although in the past few years the use of phenomenological-based models has increased in the scale-up field (2, 3, 11, 23), it encompasses a big inconvenient when validating it at several operating scales; especially because model parameters such as transfer coefficients (mass, heat and momentum) vary when scale changes (25). This fact forces the designer to use optimization algorithms for finding optimal parameters which results impractical, arduous and in a never ending task when the available process model is complex (11, 21).
As a way to overcome these drawbacks and considering that a PBSM is a fundamental tool to comprehend the behaviour of a given process, Figure 1 presents the proposed methodology for scaling up continuous processes. The fifteen steps of the procedure are described as follows.

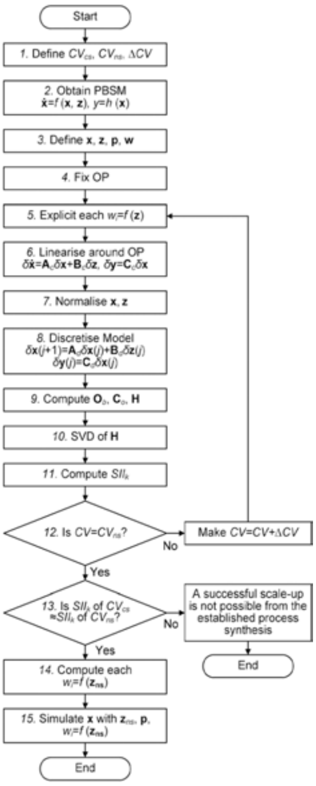

Figure 1. Scale-up proposed procedure.

Step 1: the Capacity Variable at the current scale (CV_{cs}) and new scale (CV_{ns}), and Capacity Variable step (ΔCV) are defined. Here, *CV* is any process variable indicating a processing capacity of a process unit. It is associated to hold-up or a process extensive variable, such as volume, mass, length, among others. This means that *CV* is set by the designer in order to carry out the process at the desired scale. According to this, *CV* alters all scale-dependent parameters when increasing the scale.

Step 2: a PBSM of the process is obtained using the methodology developed in (26). Considering that a model is a simplified representation of the real process, the model needs to be validated at the current scale (cs) in order to represent the process at the new scale (ns). Also, given its phenomenological structure, only the parameters determined from observed data or black-box models may add uncertainty to the representation. Of these parameters, only the scale-dependant ones need to be described by expressions valid at the *cs* and *ns*.

Step 3: state variables (**x**), design variables (**z**), synthesis parameters (**p**) and design-variables-dependent parameters (**w**) are defined from the obtained model. Definitions of **x**, **z**, **p** and **w** are given below.
State variables (**x**) are the smallest set of variables which must be specified at time $t=t_0$ in order to be able to predict the behaviour of the process for any time $t \geq t_0$ (27).
Design variables (**z**) are the variables whose values can be freely varied by the designer to define a designed process.
Synthesis parameters (**p**) are characteristic (inherent) parameters of the process, and are established from the process conception. Once established, they remain fixed during the scale-up.
Design-variables-dependent parameters (**w**) are the parameters that depend on the design variables, i.e. **w** are those parameters that can be written as an explicit function of **z**.
Here, it is worth highlighting that *CV* may also be considered as a design variable because it can be freely varied by the designer when scaling up the process.

Step 4: the Operating Point (OP) is fixed. It is important to clarify that the OP is fixed from the process synthesis and the proposed methodology does not optimizes it. Thus, this point must be properly chosen in order to carry out the scale-up task successfully. The definition of OP is given as follows.
Operating Point (OP) is a given value of **x** vector that represents a mathematical equilibrium point of the model. This means that the derivative of a given state variable x_k with respect to time t is equal to zero at the OP (3).

Step 5: an equation for each $w_i=f(\mathbf{z})$ must be found. These expressions must be valid in all scales between the *cs* and *ns*.

Step 6: it is assumed that the actual system dynamics in the immediate proximity of the OP can be approximated by the first terms of the Taylor series. Thus, the model is linearized around the OP as follows:

$$\delta\dot{\mathbf{x}} = \mathbf{A}_c\delta\mathbf{x} + \mathbf{B}_c\delta\mathbf{z} \qquad \textbf{Eq. 1}$$

$$\delta\mathbf{y} = \mathbf{C}_c\delta\mathbf{x} \qquad \textbf{Eq. 2}$$

Here, $\mathbf{A}_c$, $\mathbf{B}_c$ and $\mathbf{C}_c$ are the Jacobian matrices of the continuous system.

Step 7: $\mathbf{B}_c$ and $\mathbf{C}_c$ matrices are modified to make both design and output variables dimensionless and normalised, see Equations 3 and 4. This type of transformation, called "scaling" in (28), is commonly used when studying control systems with the aim of all process variables to be in comparable ranges. Here, the word "scaling" is avoided in order to prevent any confusion when mentioning the words "scale-up" associated to scale increments. The $\mathbf{A}_c$ matrix is not modified because the Hankel matrix is a tool that only considers the inputs and outputs of the system, so any mathematical operation done over **x** will be annulled during the Hankel matrix calculation (15).

$$\bar{b}_{ij} = b_{ij}(z_{j,\max} - z_{j,\min}) \qquad \textbf{Eq. 3}$$

$$\bar{c}_{ij} = \frac{c_{ij}}{(y_{i,\max} - y_{i,\min})} \qquad \textbf{Eq. 4}$$

The subscripts max and min are the maximum and minimum values of z_j and y_i in each case. They are established from the process synthesis based on the knowledge of the process design and desired performance targets. Here, $z_{j,min}$ and $z_{j,max}$ may depend on the scale whilst $y_{i,min}$ and $y_{i,max}$ do not depend on the scale. Also, it is considered that the system is completely observable, reason why $\mathbf{C}_c$ is the Identity matrix, so y_i and x_i limits are the same. It is worth clarifying that there are several ways to carry out the normalization of the variables. In this case, $\mathbf{B}_c$ and $\mathbf{C}_c$ matrices are transformed for normalising both design and state variables because it is a simpler procedure than constructing a dimensionless model of the process.

Step 8: the model is discretised as shown in Figure 1. For model discretisation, the sampling time (t_s) is at least 20 times lower than the response time of the fastest dynamics (15) in order to the discrete model represents the linear one.

Step 9: observability ($\mathbf{O}_b$), controllability ($\mathbf{C}_o$) and Hankel ($\mathbf{H}$) matrices are computed for the linear discrete system as shown in Equations 5, 6 and 7.

$$\mathbf{O}_b = \begin{bmatrix} \mathbf{C}_d & \mathbf{C}_d\mathbf{A}_d & \mathbf{C}_d\mathbf{A}_d^2 & \cdots & \mathbf{C}_d\mathbf{A}_d^{n_x-1} \end{bmatrix}^T \qquad \text{Eq. 5}$$

$$\mathbf{C}_o = \begin{bmatrix} \mathbf{B}_d & \mathbf{A}_d\mathbf{B}_d & \mathbf{A}_d^2\mathbf{B}_d & \cdots & \mathbf{A}_d^{n_x-1}\mathbf{B}_d \end{bmatrix} \qquad \text{Eq. 6}$$

$$\mathbf{H} = \mathbf{O}_b\mathbf{C}_o \qquad \text{Eq. 7}$$

where n_x represents the number of state variables and, $\mathbf{A}_d$, $\mathbf{B}_d$, and $\mathbf{C}_d$ are the Jacobian matrices of the discrete system. Here, observability and controllability are not considered as independent concepts because for extending the use of the Hankel matrix from control to process design, an analogy between manipulated variables (**u**) and design variables (**z**) was done. Therefore, $\mathbf{O}_b$ and $\mathbf{C}_o$ have yet to be defined and discussed in the context of process design.

Step 10: **H** is decomposed in singular values as shown in Equation 8. Here, **U** and **V** matrices are the orthonormalised eigenvectors of $\mathbf{HH}^T$ and $\mathbf{H}^T\mathbf{H}$. The diagonal elements of **S** are non-negative square roots of the eigenvalues of $\mathbf{HH}^T$ known as singular values σ_{ii}.

$$\mathbf{H} = \mathbf{USV}^T \qquad \text{Eq. 8}$$

Step 11: the State Impactability Index of each state variable (SII_k) is computed as shown in Equation 9.

$$SII_k = \sqrt{\sum_{i=1}^{n_\sigma} \sigma_{ii} \left[\sum_{j=0}^{n_x-1} U_{k+n_x j i}^2 \right]} \qquad \text{Eq. 9}$$

where n_σ is the number of singular values. SII_k represents the impactability of the process design variables (**z**) as a whole over a k-th given state variable (x_k). In this way, the main dynamics (the most impacted dynamics) is the x_k with the highest SII.

Step 12: as can be seen from Figure 1, steps five to twelve are repeated until $CV=CV_{ns}$. Within this loop **w** are computed as the operating scale is increased.

Step 13: SII_k at the current and new scale are compared. If SII_k values at the *cs* and *ns* are approximately equal, continue with the fourteenth step. On the opposite case, i.e. if at least one of SII_k values is outside the interval $[0.9\, SII_k, 1.1 SII_k]$ (**x** and hence SII_k are expected to have small changes) a successful scale-up is not possible from the established process synthesis. Therefore, the process synthesis must be reviewed.

Step 14: each w_i is computed as a function of $\mathbf{z}_{ns}$ in order to establish the scaled unit design.

Step 15: the process is simulated with **p**, $\mathbf{z}_{ns}$ and $\mathbf{w}_{ns}$ for verifying if the scale-up task was properly done.

A BRIEF ILLUSTRATIVE EXAMPLE

Consider the CSTR shown in Figure 2, where a free-radical polymerization of methyl methacrylate (MMA) takes place, with azo-bis-isobutyronitrile (AIBN) as initiator and toluene as solvent. Here, the jacket removes heat generated by the reaction.

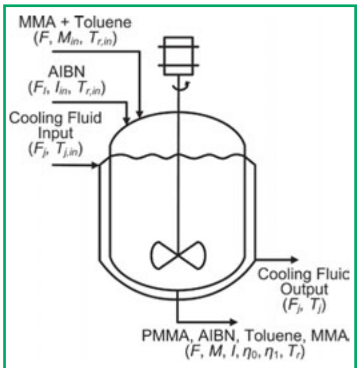

Figure 2. Polymerization process flow diagram.

In Figure 2, *M* and *I* represent monomer and initiator concentration respectively, η_0 and η_1 represent zero and first moments of the dead polymer respectively, T_r represents reactor temperature and T_j represents jacket temperature. Also, F, F_I and F_j represent monomer, initiator and cooling fluid flow rates respectively. In addition, subscript *in* represents inlet streams. Each one of the fifteen steps of the previously stated procedure is performed as follows.

Step 1: $CV_{cs}=0.1m^3$, $CV_{ns}=1m^3$ and $\Delta CV=0.1m^3$ are defined.

Step 2: a model of the process is obtained. Equations 10, 11, 12, 13, 14 and 15 describe the reactor dynamic behaviour (29).

$$\frac{dM}{dt} = -(k_p + k_{fm})MP_0 + \frac{F(M_{in} - M)}{V_r} \qquad \text{Eq. 10}$$

$$\frac{dI}{dt} = -k_I I + \frac{F_I I_{in} - FI}{V_r} \qquad \text{Eq. 11}$$

$$\frac{d\eta_0}{dt} = (0.5k_{tc} + k_{td})P_0^2 + k_{fm}MP_0 - \frac{F\eta_0}{V_r} \qquad \text{Eq. 12}$$

$$\frac{d\eta_1}{dt} = M_{W,m}(k_p + k_{fm})MP_0 + \frac{F\eta_1}{V_r} \qquad \text{Eq. 13}$$

$$\frac{dT_r}{dt} = \frac{k_p MP_0 \Delta H_p}{C_{p,r}\rho_r} - \frac{U_r A_i (T_r - T_j)}{C_{p,r}\rho_r V_r} + \frac{F(T_{r,in} - T_r)}{V_r} \qquad \text{Eq. 14}$$

$$\frac{dT_j}{dt} = \frac{F_j(T_{j,in} - T_j)}{V_j} + \frac{U_r A_i (T_r - T_j)}{C_{p,j}\rho_j V_j} \qquad \text{Eq. 15}$$

Here, P_0 represents zero moment of the live polymer, given by Equation 16. k_p, k_{fm}, k_I, k_{tc} and k_{td} are kinetic constants, computed from an Arrhenius type equation as shown in Equation 17. Also, the number average molecular weight of the polymer (M_n) is computed from Equation 18. Given that M_n is strongly related to functional properties of the polymer such as particles size, rigidity, chemical resistance, thermal stability, among others, this work seeks to maintain its value when scaling up the process.

$$P_0 = \left[\frac{2fk_I I}{k_{td} + k_{tc}}\right]^{0.5} \qquad \text{Eq. 16}$$

$$k_j = k_{j0} e^{\frac{E_j}{R_g T_r}} \qquad \text{Eq. 17}$$

$$M_n = \frac{\eta_0}{\eta_1} \qquad \text{Eq. 18}$$

In addition, *f* is the efficiency of the initiator, V_r represents reactor volume, $M_{W,m}$ represents monomer molecular weight, ρ_r and ρ_j are reactor and jacket fluids densities, $C_{p,r}$ and $C_{p,j}$ are the specific heat capacities of reactor and jacket fluids, ΔH_p is the heat of polymerization, U_r represents the overall heat-transfer coefficient and A_i is the heat-transfer area.

Step 3: **x**, **z**, **p** and **w** are defined from the model as shown in Equations 19, 20, 21 and 22.

$$\mathbf{x} = \left[M \quad I \quad \eta_0 \quad \eta_1 \quad T_r \quad T_j\right] \qquad \text{Eq. 19}$$

$$\mathbf{z} = \left[V_r \quad M_{in} \quad I_{in} \quad T_{r,in} \quad T_{j,in}\right] \qquad \text{Eq. 20}$$

$$\mathbf{p} = \left[k_{j0} \quad E_j \quad R_g \quad M_{W,m} \quad f \quad \rho_r \quad \rho_j \quad C_{p,r} \quad C_{p,j} \quad \Delta H_p \quad \tau_I \quad \tau_m \quad \tau_j\right] \qquad \text{Eq. 21}$$

$$\mathbf{w} = \left[V_j \quad F \quad F_I \quad F_j \quad U_r \quad A_i\right] \qquad \text{Eq. 22}$$

where τ_I , τ_m and τ_j represent residence times of the initiator, monomer and cooling fluid respectively.

Step 4: the value for the OP at the current scale is fixed, as can be seen from Table 1. Here, OP, **z**, **w**, **p** values at *cs* were taken from (29). Also, M_{in}, I_{in}, $T_{r,in}$ and $T_{j,in}$ values are set in their *cs* values.

Symbol	Value	SI Unit
M	5.5	$kmol/m^3$
I	1.3×10^{-1}	$kmol/m^3$
η_0	2.0×10^{-3}	$kmol/m^3$
η_1	4.9×10^{1}	kg/m^3
T_r	335	K
T_j	297	K

Table 1. Operating Point for $0.1m^3$ reactor (29).

Step 5: an equation of each w_i is established as shown in Equations 23, 24, 25 and 26. In this case, Equation 23 is a heuristic rule for chemical reactors design taken from (29).

$$V_j = \frac{1}{5} V_r \qquad \text{Eq. 23}$$

$$F = \frac{V_r}{\tau_m} \qquad \text{Eq. 24}$$

$$F_I = \frac{V_r}{\tau_I} \qquad \text{Eq. 25}$$

$$F_j = \frac{V_j}{\tau_j} \qquad \text{Eq. 26}$$

In addition, considering that most of the traditional scale-up methods involve the fulfilment of the geometrical similarity as a primary criterion when scaling up chemical processes (3, 5, 6, 21), two cases are considered for U_r calculation: i) the overall heat-transfer coefficient available ($U_{r,a}$) and ii) the overall heat-transfer coefficient required ($U_{r,r}$). For the former, the process is scaled-up maintaining the geometrical similarity, that keeps the overall heat-transfer coefficient fixed by the current scale design. For the latter, the overall heat-transfer coefficient is computed from the process energy requirements without fixing the geometry of the reactor. This comparison allows establishing the effect of designing a geometrically similar unit instead of the required by the process dynamics.

$$U_{r,a} = \frac{1}{\frac{1}{h_i} + \frac{\delta}{k_w}\frac{A_i}{A_w} + \frac{1}{h_j}\frac{A_i}{A_o}} \qquad \text{Eq. 27}$$

$$U_{r,r} = -\frac{F_j \rho_j C_{p,j}}{A_i}\left[\frac{T_{j,in}\big|_{ss} - T_j\big|_{ss}}{T_r\big|_{ss} - T_j\big|_{ss}}\right] \qquad \text{Eq. 28}$$

A_i, A_w and A_o are the inside, wall and outside heat-transfer areas respectively. For $U_{r,a}$ calculation, a standard cylindrical geometry for computing the heat-transfer areas (A_i, A_w, A_o), a ratio of the impeller to the tank diameter of D/T=1/3 and a ratio of the liquid level to the tank diameter of Z/T=1 are considered. h_i and h_j are the inner (process side) and outer (cooling fluid side) heat-transfer coefficients, computed with Equations 29 and 30 respectively. δ and k_w are the vessel wall thickness and thermal conductivity respectively (30).

$$h_i = 0.74\frac{k_r}{T}\left[\frac{D^2 N \rho_r}{\mu_r}\right]^{2/3}\left[\frac{C_{p,r}\mu_r}{k_r}\right]^{1/3}\left[\frac{\mu_r}{\mu_{w,r}}\right]^{0.14} \qquad \text{Eq. 29}$$

$$h_j = 0.027\frac{k_j}{D_e}\left[\frac{D_e \rho_j F_j}{A_x \mu_j}\right]^{4/5}\left[\frac{C_{p,j}\mu_j}{k_j}\right]^{1/3}\left[\frac{\mu_j}{\mu_{w,j}}\right]^{0.14} \qquad \text{Eq. 30}$$

$$A_x = \frac{\pi}{2}\left[D_{jo} - D_{ji}\right] \qquad \text{Eq. 31}$$

$$D_e = \frac{D_{jo}^2 - D_{ji}^2}{D_{ji}} \qquad \text{Eq. 32}$$

$$N = N_{cs}\left[\frac{D_{cs}}{D}\right]^{2/3} \qquad \text{Eq. 33}$$

where A_x, D_e and *L* are the cross-sectional flow area, heat-transfer equivalent diameter and jacket passage length respectively. *N* is the agitator speed and, *μ* and *k* are the fluids viscosity and thermal conductivity respectively. D_{ji} and D_{jo} are inner and outer diameter of the annular jacket.

Step 6: the model is linearised around OP as shown in Equations 1 and 2.

Step 7: $\mathbf{B}_c$ and $\mathbf{C}_c$ matrices are modified as shown in Equations 3 and 4, considering that $y_{i,min}$ and $y_{i,max}$ are computed as the ±10 percent of their nominal values at the *cs*, since minor changes are expected for these variables when increasing the scale, especially because by using the proposed methodology the dynamic behaviour of the process at the *cs* is transferred to the *ns*. Here, $z_{j,min}$ and $z_{j,max}$ are also computed as the ±10 percent of their nominal values at the *cs*, making an exception for maximum and minimum limits of V_r, which are computed as the ±10 percent of its nominal value at each operating scale. In this case, V_r is both a design variable and the *CV*.

Step 8: the model is discretised with t_s=0.02s according to Shannon's sampling theorem.

Step 9: the observability ($\mathbf{O}_b$), controllability ($\mathbf{C}_o$), and Hankel (**H**) matrices are computed as shown in Equations 5, 6 and 7 with n_x=6.

Step 10: **H** is decomposed in singular values using Equation 8.

Step 11: *SII* of each x_k is computed by means of Equation 9, with n_σ=6 (determined as Hankel Matrix rank).

Step 12: as can be seen from Figure 1, steps five to twelve are repeated until $CV=CV_{ns}$. During this loop **w** are computed whilst increasing the scale. Figure 3 shows a comparison for the *SII* of η_0 for both cases, i.e. using $U_{r,r}$ and $U_{r,a}$. Here, only the evolution of η_0 when increasing the scale is shown in Figure 3 because it corresponds to the main dynamics of the process. Additionally, Table 2 summarizes the *SII* values for all the state variables at *cs* and *ns*.

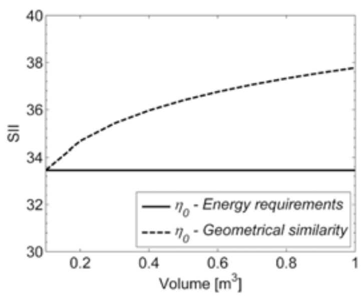

Figure 3. State Impactability Index for η_0 when increasing CV.

From Figure 3, it can be seen that as the operating scale increases when the geometrical similarity is held the *SII* value also increases. This fact shows that by scaling up the process using $U_{r,a}$ the process dynamic behaviour degrades. This behaviour can also be seen from Table 2 for all the state variables.

Step 13: as can be seen from Table 2 for both cases, the SII_k values are compared at the current and new scale.

Variable	SII_{cs}	SII_{ns} using $U_{r,r}$	SII_{ns} using $U_{r,a}$
M	1.85	1.85	2.08
I	0.60	0.60	0.63
η_0	33.46	33.46	37.78
η_1	19.98	19.98	22.58
T_r	1.01	1.01	1.21
T_j	0.88	0.88	0.91

Table 2. State Impactability Index values at 0.1m^3 and 1m^3.

From Table 2, it can also be seen that the *SII* values remain constant when using $U_{r,r}$ and change when using $U_{r,a}$, indicating that the process behaviour degrades when scaling up the process maintaining the geometrical similarity. Here, *SII* values for $\eta0>\eta1>M>Tr>Tj>I$, meaning that η_0 is the most impacted dynamics by the design variables of the process. Also, as M_n is function of η_0 (the total dead polymer concentration), see Equation 18, when scaling up the process using $U_{r,a}$ an alteration in M_n must be expected.

Step 14: as can be seen from Table 3, $w_i=f(\mathbf{z_{ns}})$ at the OP are computed. Here, it can be seen that a smaller value for the overall heat-transfer coefficient is computed when using $U_{r,a}$ than $U_{r,r}$, this means that a smaller process unit than the required one was designed.

Symbol	$w_i\|_{cs}$	$w_i\|_{ns}$ using $U_{r,r}$	$w_i\|_{ns}$ using $U_{r,a}$	SI Unit
V_j	0.02	0.2	0.2	m^3
F	1.0	10.0	10.0	m^3/h
F_I	0.0168	0.168	0.168	m^3/h
F_j	3.263	32.63	32.63	m^3/h
U_r	1,449	3,122	1,876	kJ/m^2hK
A_i	0.994	4.613	4.613	m^2

Table 3. Design-variables-dependent parameters values at 0.1m^3 and 1m^3.

Considering that U_r must be 3,122 kJ/m^2hK at the *ns*, a new jacket geometry is proposed. Here, Equations 34, 35 and 36 are used (30) to satisfy the heat-transfer demand (U_r) at the *ns*. Therefore, two baffles are added to the annular jacket. From here $U_{r,r}$ is computed using Equation 27, with h_i given by Equation 29 and h_j by Equation 34.

$$h_j = 0.027\frac{k_j}{D_e}\left[\frac{D_e\rho_j F_j}{A_x\mu_j}\right]^{4/5}\left[\frac{C_{p,j}\mu_j}{k_j}\right]^{1/3}\left[\frac{\mu_j}{\mu_{w,j}}\right]^{0.14}\left[1+3.5\frac{D_e}{D_c}\right] \quad \text{Eq. 34}$$

$$D_e = 2\left|D_{jo}-D_{ji}\right| \quad \text{Eq. 35}$$

$$A_x = p_b\left[\frac{D_{jo}-D_{ji}}{2}\right] \quad \text{Eq. 36}$$

where D_c is the centre line diameter of the annular jacket and p_b is the position of each baffle.

Step 15: the process is simulated with **p**, $\mathbf{z_{ns}}$ and $\mathbf{w_{ns}}$ values. As it was mentioned before, changes in *SII* values with scale increments show a process behaviour degradation, this is the reason why, in Table 4, the state variables values at OP are compared for the proposed design and maintaining the geometrical similarity at the *ns*.

Symbol	x_{ns} using $U_{r,r}$	x_{ns} using $U_{r,a}$	SI Unit
M	5.5	1.3	$kmol/m^3$
I	1.3×10^{-1}	5.0×10^{-4}	$kmol/m^3$
η_0	2.0×10^{-3}	5.2×10^{-1}	$kmol/m^3$
η_1	4.9×10^{1}	4.7×10^{2}	kg/m^3
T_r	335	430	K
T_j	297	301	K

Table 4. Comparison of the Operating Point at 1m^3.

By comparing Table 1 and Table 4, it can be seen that it is not possible to reproduce the same OP at the *ns* by maintaining the geometrical similarity. Also, it can be seen that by holding the dynamics hierarchy the same OP from the *cs* is obtained at the *ns*. In addition, Figure 4 shows a comparison of M_n at the *cs* and *ns* for both cases.

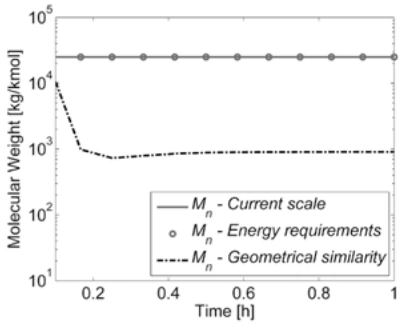

Figure 4. Comparison of the number average molecular weight of the polymer at 0.1m^3 and 1m^3.

It can be seen that $M_{n,cs}\approx M_{n,ns}$=25,000*kg/kmol* using $U_{r,r}$ and that $M_{n,cs}\neq M_{n,ns}$=907*kg/kmol* using $U_{r,a}$ when the system reaches steady state. This shows that geometrical similarity criterion is not always the best option when scaling up chemical processes and, that by means of the proposed procedure the same M_n from the *cs* is achieved at *ns*.

CONCLUSIONS

The main contribution of this work is the integration of an index (*SII*) to the scale-up of continuous reactors, which allows the establishment of the real scale factors of a process, holding the same dynamics hierarchy when changing the operating scale.

Here, the use of the Hankel matrix for analysing the process dynamics and establishing the effect of the design variables ($\mathbf{z}$) as a whole over each state variable (x_k) is the key for carrying out a successful scale-up.

A non-isothermal MMA solution polymerization CSTR is scaled-up from $0.1m^3$ to $1m^3$. As a result of this, the scale factors for maintaining the same OP at the new scale were found. Here, it is also found that the most impacted dynamics by the design variables is the total dead polymer concentration and the less impacted one is the initiator concentration. In addition, considering that traditional scale-up methods involve the fulfilment of the geometrical similarity, from this example, it is also illustrated that traditional scale-up methods do not always lead into the best commercial unit design. Here, if the geometrical similarity is held other parameters of the process need to be changed in order to achieve the same performance targets set at the current scale.

REFERENCES AND NOTES

1. Donati G., Paludetto R., *Catal. Today*, **34(3-4)**, 483-533 (1997).
2. Lonsane B.K., Saucedo-Castaneda G., et al., *Process Biochem.*, **27(5)**, 259-273 (1992).
3. Ruiz A.A., Alvarez H., *Inf. Tecnol.*, **22(6)**, 33-52 (2011).
4. Brooks B.W., *Chem. Eng. Technol.*, **33(11)**, 1737-1744 (2010).
5. Inglezakis V.J., Poulopoulos S.G., *Reactors scale-up*, in *Adsorption, Ion Exchange and Catalysis Design of Operations and Environmental Applications*. Elsevier: Amsterdam, The Netherlands. p. 523-550 (2006).
6. Ruzicka M.C., *Chem. Eng. Res. Des.*, **86(8)**, 835-868 (2008).
7. Zlokarnik M., *Scale-Up in Chemical Engineering*. 2nd Ed., Weinheim: Wiley-VCH Verlag GmbH & Co. KGaA. 271-271 (2006).
8. Meyer T., *Org. Process Res. Dev.*, **7(3)**, 297-302 (2003).
9. Ranade V.V., Chaudhari R.V., et al., *Reactor Performance and Scale-Up*, in *Trickle Bed Reactors: Reactor Engineering & Applications*. Elsevier: Amsterdam. p. 171-210 (2011).
10. Pollard D.J., Kirschner T.F., et al., *Biotechnol. Bioeng.*, **96(2)**, 307-317 (2007).
11. Garcia-Ochoa F., Gomez E., *Biotechnol. Adv.*, **27(2)**, 153-176 (2009).
12. Papagianni M., *J. Microb. Biochem. Technol.*, **S5(001)**, 1-7 (2011).
13. Choo Y., *IEICE T. Fund. Electr.*, **E88–A(12)**, 3658-3660 (2005).
14. Sreeram V., Zomaya A.Y., *Electron. Lett.*, **27(4)**, 362-364 (1991).
15. Alvarez L.A., Espinosa J.J., *CLCA 2013*, ISBN 9801112247 (2008).
16. Sweere A.P.J., Luyben K.C.A.M., et al., *Enzyme Microb. Technol.*, **9(7)**, 386-398 (1987).
17. Coker A.K., *Scale-Up in Reactor Design*, in *Modeling of Chemical Kinetics and Reactor Design*. Gulf Professional Publishing: Woburn. p. 1034-1081 (2001).
18. Johnstone R.E., Thring, M.W., *Pilot Plants, Models and Scale-up Methods in Chemical Engineering*. New York: McGraw-Hill. 307-307 (1957).
19. Leckner B., Szentannai P., et al., *Fuel*, **90(10)**, 2951-2964 (2011).
20. Rüdisüli M., Schildhauer T.J., et al., *Powder Technol.*, **217(0)**, 21-38 (2012).
21. Bisio A., Kabel R.L., *Scaleup of Chemical Processes Conversion from Laboratory Scale Tests to Successful Commercial Size Design*. New York: John Wiley & Sons, Inc. 699-699 (1985).
22. Chan N., Cunningham M.F., et al., *Macromol. Rapid Commun.*, **32(7)**, 604-609 (2011).
23. Fathi Roudsari S., Ein-Mozaffari F., et al., *Chem. Eng. J.*, **219(0)**, 429-442 (2013).
24. Dudukovic M.P., *Chem. Eng. Sci.*, **65(1)**, 3-11 (2010).
25. Caygill G., Zanfir M., et al., *Org. Process Res. Dev.*, **10(3)**, 539-552 (2006).
26. Alvarez H., Lamanna R., et al., *Rev. Iberoam. Autom. Inform. Ind.*, **6(3)**, 10-20 (2009).
27. Kalman R.E., *IRE Trans. Autom. Control*, **4(3)**, 110-110 (1959).
28. Skogestad S., Postlethwaite I., *Multivariable feedback control: analysis and design*. Vol. 2. Wiley New York (2007).
29. Daoutidis P., Soroush M., et al., *AIChE J.*, **36(10)**, 1471-1484 (1990).
30. Bondy F., Lippa S., *Chem. Eng.*, **90(7)**, 62-71 (1983).

tks
tekno
scienze
publisher

6TH SYMPOSIUM ON CONTINUOUS FLOW REACTOR TECHNOLOGY FOR INDUSTRIAL APPLICATIONS

2014

Budapest, 23-25 September

+ optional half-day practical session (26 Sept)

After the really big success of our first four simposia held In Madrid, Paris, Como, Lisbon and Pisa here we are again for the sixth year and, once again, we have the pleasure to invite you to the new edition of this event.
This year we will meet in the historical city of Budapest - Hungary.
A suggestive location for our unbeatable social events...
...a GREAT OPPORTUNITY for NETWORKING!

The 6th Symposium will consist of 1 day training course (23 Sept), 2 days conference (24-25 Sept) and an optional half-day practical session (limited places) (26 Sept).

Sponsorship opportunities:

Simona Rivarollo - **simona@teknoscienze.com**

Scientific contents:

Dr Gayle De Maria - **gayle@teknoscienze.com**

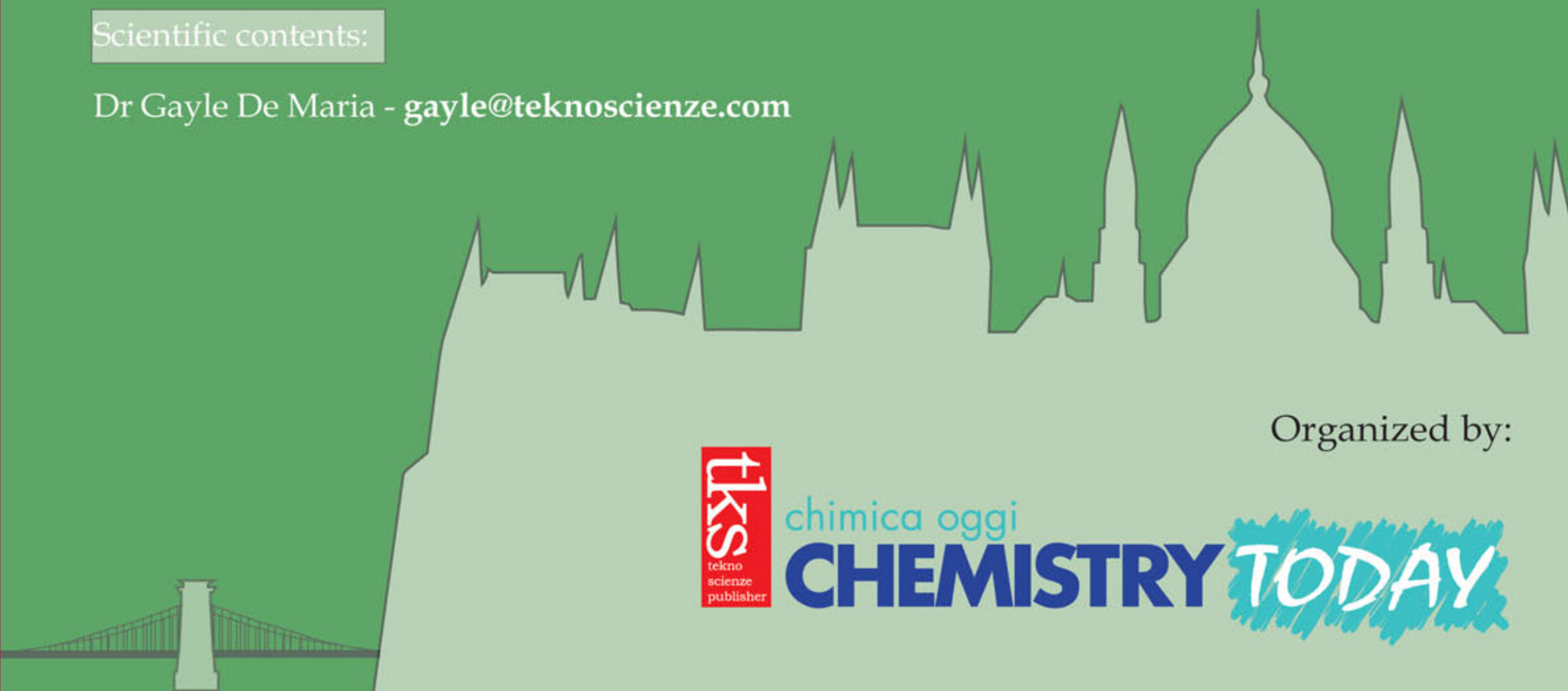

Organized by:

tks
tekno
scienze
publisher

chimica oggi
CHEMISTRY TODAY